https://doi.org/10.5194/egusphere-2024-2652
Preprint. Discussion started: 15 October 2024

Thermal diffusivity of permafrost in the Swiss Alps determined from borehole temperature data

Samuel Weber[1,2] and Alessandro Cicoira[3,4]

[1]WSL Institute for Snow and Avalanche Research SLF, Davos, Switzerland
[2]Climate Change, Extremes and Natural Hazards in Alpine Regions Research Center CERC, Switzerland
[3]Department of Geography, University of Zurich, Switzerland
[4]GEOTEST AG, Zollikofen, Bern, Switzerland

Correspondence: Samuel Weber (samuel.weber@slf)

Abstract. Mountain permafrost is warming and thawing globally due to climate change. Its mechanical properties largely depend on ground temperature, whereby the primary process of heat transfer in frozen ground is heat conduction. Thermal diffusivity quantifies the rate of heat propagation in a material and is thereby a key thermal property, but no empirical values for mountain permafrost substrates are currently available. In this study, we derive the thermal diffusivity of different mountain permafrost landforms and substrates in the Swiss Alps empirically for the first time. To do so, we perform a linear regression analysis of the heat diffusion equation and validate the derived thermal diffusivity with inversions of numerical and analytical solutions. As a data basis, we systematically analyze data from the 29 temperature boreholes of the Swiss Permafrost Monitoring Network PERMOS, which allows us to investigate the natural variability of thermal diffusivity in space and time and derive a well-constrained range of thermal diffusivity in mountain permafrost (25- to 75-percentile range: $1.1 - 3.3\,\mathrm{mm^2\ s^{-1}}$) and the overlying active layer (25- to 75-percentile range: $0.8 - 2.4\,\mathrm{mm^2\ s^{-1}}$). While we find only small but significant ($p < 0.01$) differences in diffusivity between the landforms for all three approaches, strong spatio-temporal variations are identified. Our results complement our understanding of the thermal properties of permafrost and thus directly offer potential implications for the development and application of new ground temperature and energy-balance models. Furthermore, we discuss the potential to indirectly identify short-term non-conductive heat fluxes by isolating discrepancies between observations and model predictions of temperature rate variations with time. The quantification of non-conductive heat fluxes is still poorly constrained due to their strongly non-linear nature and the inherent challenges in their measurement. Non-conductive heat fluxes point to the presence of water and/or air circulation in the permafrost. Water can significantly influence the mechanical properties of permafrost substrates. The dynamics of unstable slopes are increasingly being driven by water infiltration related to ice loss within the permafrost. Therefore, our method and results open new possibilities in permafrost science, hydrogeology, natural hazard studies, and practical applications such as high-mountain construction technology.

1 Introduction

Permafrost is defined in purely thermal terms, irrespective of water and/or ice content or lithological composition. It is a natural substrate that remains at or below $0°C$ for at least two consecutive years (Muller, 1945). An active layer, a few meters of

https://doi.org/10.5194/egusphere-2024-2652
Preprint. Discussion started: 15 October 2024

seasonally frozen and thawed ground, typically forms the interface between the permafrost and the atmosphere. The thermodynamics of the active layer are complex, as this layer can consist of both bedrock and often a multiphase mixture (i.e., rock of different sizes, ice, water, and air), whereby several processes, such as conductive, advective, and convective heat flows, determine the energy balance (e.g., Hanson and Hoelzle, 2004; Scherler et al., 2014; Wicky and Hauck, 2017). The acting heat exchange processes are strongly influenced by the site-specific physical properties of the rock itself but also by external influencing factors such as the thickness of the snow cover, which has an insulating effect but also favors water infiltration (Bonnaventure and Lamoureux, 2013). The heat balance of the inner core (permafrost body) is expected to be primarily controlled by heat conduction (Haeberli et al., 2006). Here at depth, once water is present, the thermal regime of the permafrost favors the formation and preservation of ground ice (Taber, 1930; Murton and French, 1994), unless the temperature is close to 0°C (Bast et al., 2024), pressurized water flow occurs (Offer et al., 2024) or in the presence of fine-grained sediments (i.e. clay) where unfrozen water contents can be high (Williams, 1964).

Permafrost reacts sensitively to climate-induced increasing air temperatures (IPCC, 2022) and is currently experiencing strong warming, evidenced through a globally measured borehole temperature increase of 0.3°C between 2007 and 2016 (Biskaborn et al., 2019). The warming and thawing of permafrost can accelerate the release of large quantities of organic carbon currently stored in high-latitude regions of the Earth, thus accelerating climate change (Schuur et al., 2015; Strauss et al., 2024). In cold mountain areas, permafrost is abundant in rock slopes at high elevations within different landforms, such as bedrock, talus slopes, and rock glaciers. Long-term temperature time series also show a sustained warming and active layer thickening trend across the European Alps (Haberkorn et al., 2021; Pogliotti et al., 2023; Magnin et al., 2024). This warming influences the mechanical properties of rock and ice in the ground (Krautblatter et al., 2013), alters physical rock matrix properties (Draebing and Krautblatter, 2012), and affects the hydraulic regime in the rock mass (Haeberli et al., 1997). The hydraulic permeability is much lower in rock masses with frozen and ice-filled fractures than in unfrozen ones, and perched water often results in high pressure (Pogrebiskiy and Chernyshev, 1977). Still, water from the surface, either precipitation or snow melt, can percolate through cracks into the active layer and advect heat to the ice level much more efficiently than is possible via pure conduction, potentially forming thawing corridors (Krautblatter and Hauck, 2007; Magnin and Josnin, 2021). However, apart from some rock glacier-specific studies (e.g., Cicoira et al., 2019b; Kenner et al., 2020; Cicoira et al., 2021; Marcer et al., 2021; Phillips et al., 2023; Bast et al., 2024), minimal data about the presence and quantity of water in mountain permafrost are available, and only a few in-situ measurements or laboratory experiments (e.g., Mellor, 1973; Hasler et al., 2011; Draebing and Krautblatter, 2012; Jia et al., 2015) characterize the physical properties of frozen ground.

Generally, the ground's thermal regime and thermodynamic behavior are mainly characterized by different processes such as phase change, heat conduction (diffusion) or non-conductive heat transfer, and the material's thermal properties. While thermal diffusivity quantifies the rate of heat propagation in a material and, therefore, is the one petrophysical parameter relevant in diffusive and stationary models (Yershov, 1998), arbitrary values are used and they are often assumed to be constant in time and depth (e.g. Magnin et al., 2017; Marcer et al., 2024). To our knowledge, only limited site-specific, empirically derived diffusivity values for the near-surface active layer are available (i.e., based on the analytical solutions of the heat conduction

https://doi.org/10.5194/egusphere-2024-2652
Preprint. Discussion started: 15 October 2024

equation for data from Matterhorn and Aiguille du Midi, Pogliotti et al., 2008), but none at all for the underlying permafrost nor any characterization of the spatio-temporal variation.

To address this gap, this study empirically derives thermal diffusivity in mountain permafrost in the Swiss Alps and characterizes its natural variability in space and time for the first time. Based on the 29 borehole temperature time series of the Swiss Permafrost Monitoring Network (PERMOS, 2024), we perform statistical analysis (Nicholson and Benn, 2013) and determine the thermal diffusivity, i.e. the coefficient of the heat conduction equation (Eq. 3) through a simple Linear Regression Model (sLRM) along the borehole temperature profiles at different depths and over time. In addition, we calculate the thermal diffusivity by inverting both the numerical and analytical solution of the heat conduction equation (Cicoira et al., 2019a; Pogliotti et al., 2008).

With these three mathematically independent methods, the systematic analysis of the PERMOS borehole temperature data allows us to derive a well-constrained range for the thermal diffusivity values in mountain permafrost under natural conditions, with specific values for bedrock, talus slopes, and ice-rich rock glaciers. On the one hand, they provide realistic boundary conditions in space and time for any thermodynamical models for different mountain permafrost landforms. On the other, they enable the investigation of non-conductive processes governed by thawing and/or water advection at any location with a borehole equipped with temperature sensors. Given the one-dimensional heat conservation equation, we suggest identifying the occurrence of short-term non-conductive heat fluxes – a proxy for water or air circulation – by comparing the observed and modeled temperature changes over time and isolating spatio-temporal anomalies in the thermal diffusivity. Overall, the three modeling approaches implemented in Python (Weber, 2024) represent the diffusivity in an arbitrary subsurface and are, therefore, principally applicable to any borehole temperature profile, regardless of the ground material.

2 Data and methods

2.1 Borehole temperatures in mountain permafrost

We use the 29 PERMOS borehole temperature time series (PERMOS, 2024) to infer thermal diffusivities in mountain permafrost in the Swiss Alps. The boreholes have a depth of between 14 and 100 m and are located at 15 sites (see Fig. 1a), which consist of the different landforms bedrock, talus slopes, and rock glaciers (see Fig. 1b). A detailed description of all PERMOS boreholes is given in PERMOS (2019). This study uses the cleaned and daily aggregated data from the start of measurement until 1 June 2023 (PERMOS, 2024). The data availability and the temporal evolution of the thermal regime at the Murtèl-Corvatsch 2015 borehole (COR_0315) is exemplarily illustrated in Figure 1c-d.

2.2 Quantifying thermal diffusivity

Heat transfer by conduction in solids describes thermal energy transfer through a medium with a temperature gradient. Changes in heat conduction over time and in space can be expressed as (Fourier, 1822)

$$\frac{\partial T}{\partial t} = \kappa \nabla^2 T, \tag{1}$$

https://doi.org/10.5194/egusphere-2024-2652
Preprint. Discussion started: 15 October 2024

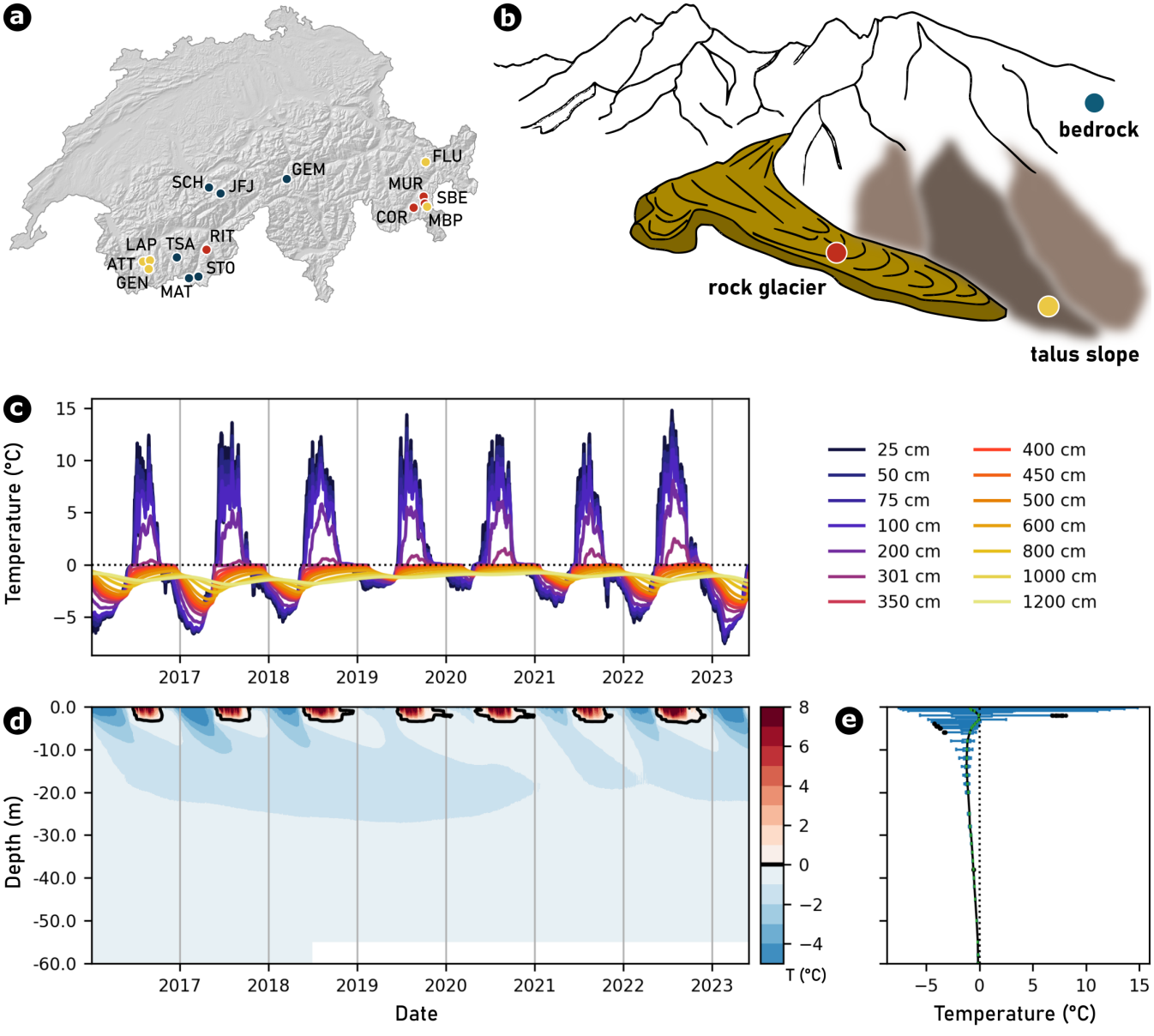

Figure 1. (a) Map of Switzerland providing an overview of the 15 PERMOS field sites with three-character abbreviations and colors referring to the type of landform. (b) A schematic visualization of three typical landforms: bedrock, talus slope, and rock glacier. As an illustrative example, (c) temperature time series for selected depths, (d) temperature contour plot for entire depth, and (e) temperature profile at Murtèl-Corvatsch 2015 (COR_0315) borehole.

https://doi.org/10.5194/egusphere-2024-2652
Preprint. Discussion started: 15 October 2024

where T is the perturbation of the temperature, ∇^2 the Laplace operator and κ the thermal diffusivity, i.e. the heat conduction coefficient.

The essential thermal properties in the ground are the specific heat capacity c [J kg^{-1} K^{-1}] describing the quantity of heat needed to increase a unit mass (1 kg) by 1 K and the thermal conductivity k [W m^{-1} K^{-1}] being a measure of how well a material transfers heat. Thermal diffusivity κ [m^2 s^{-1}] couples density ρ [kg m^{-3}] with the aforementioned thermal properties

$$\kappa = \frac{k}{\rho c}. \tag{2}$$

It measures the ability of a material to conduct thermal energy relative to its ability to store thermal energy and thereby quantifies the rate of heat propagation in a material; in other words, it measures how quickly a material reacts to temperature changes. Thermal diffusivity is thereby a key property as its influence on thermal behavior is essential for understanding and predicting heat transfer processes. As each of these thermal properties (see Eq. 2) can vary with temperature, we expect apparent variations in thermal diffusivity in mountain permafrost in space and time, for example due to changes in water content and the physical state of water. Table 1 provides an overview of the thermal properties of the end-range elements and shows the great variability that occurs in nature.

Table 1. Thermal properties of selected end-range elements, rock types, and minerals. (References: Blackwell and Steele, 1989; Clauser and Huenges, 1995; Waples and Waples, 2004; Haigh, 2012; Labus and Labus, 2018; Jia et al., 2019)

Material	Density kg m^{-3}	Specific heat capacity J g^{-1} K^{-1}	Thermal conductivity W m^{-1} K^{-1}	Thermal diffusivity mm^2 s^{-1}
Water	1000	4.184	0.6	0.14
Ice[a]	917	1.741 - 2.097	2.10 - 2.76	1.09 - 1.73
Air	1.2	1.006	0.02	16.57
Siltstone[b]	2680	0.91	0.80 - 1.25	0.33 - 0.51
Sandstone[b]	2640	0.775	2.50 - 4.20	1.22 - 2.05
Quartz[b]	2648	0.74	6.5–11.3	3.32 - 5.77
Granite[b]	2650	0.60	2.12 - 3.12	1.33 - 1.96

[a] The values for the specific heat capacity as well as the thermal conductivity of ice are temperature-dependent and specified for temperatures at -50°C and 0°C, respectively. [b] Both the values for the specific heat capacity and the thermal conductivity are sensitive to density but also to moisture content.

Assuming that heat flows by conduction only in the vertical direction (i.e. perpendicular to the ground surface) and using the resulting simplified heat conduction equation in the differential form (Carslaw and Jaeger, 1959)

$$\frac{\partial T}{\partial t} = \kappa \frac{\partial^2 T}{\partial z^2}, \tag{3}$$

https://doi.org/10.5194/egusphere-2024-2652
Preprint. Discussion started: 15 October 2024

we designed a suite of empirical models to quantify thermal diffusivity κ in mountain permafrost solely through heat conduction. Convective/advective heat flows and phase changes are not included in this equation and are, therefore, not considered in the proposed modeling approaches. Using temperature profile time series from boreholes, we perform statistical analysis (simple Linear Regression Model, Nicholson and Benn, 2013) to infer thermal diffusivity (coefficient of the heat conduction equation Eq. 3) and validate the results obtained through numerical modeling (Cicoira et al., 2019a) and analytical solution (Pogliotti et al., 2008). In each modeling approach, iterating along the profiles, we consider three adjacent temperature sensors and assign the derived thermal diffusivity values to the middle one. We apply different numerical techniques to the discrete depth and temperature values to compute the first and second derivatives along the profile for each sensor: $\frac{\partial T}{\partial z}$ using the central difference based on the depths of the neighboring sensors and taking into account the actual distances, and $\frac{\partial^2 T}{\partial z^2}$ by their finite differences. While we perform statistical and numerical modeling for each sensor depth in a one-month window that iterates by one day, we apply the analytical modeling approach only for each calendar year. The performance and representativeness of the sLRM and the numerical model are exemplarily illustrated in Figure 2, whereby both approaches fail during periods characterized by phase change (e.g., during the spring and autumn zero curtains in the active layer) or non-conductive heat fluxes (see Fig. A3, p. 20).

Statistical analysis For the statistical analysis, we considered the approach by Nicholson and Benn (2013) with parts of the analysis code by Petersen (2022). At each middle sensor of three consecutive sensors along the profile, taking into account the actual spacing and considering all data within the day-by-day iterating two-month window, we used a simple Linear Regression Model (sLRM) between the temperature Laplacian ($\frac{\partial^2 T}{\partial z^2}$, second derivative of temperature with depth between the upper and lower sensors) and the temperature change rate ($\frac{\partial T}{\partial z}$, first derivative of temperatures with time applied at the middle sensor) to determine the thermal diffusivity (i.e., heat conduction coefficient of Eq. 3) for the depth of the middle sensor. The sensor and position errors do not influence the error associated with κ as long as they are constant over time, which is assumed to be the case (Conway and Rasmussen, 2000). In contrast to the multiple linear regression model (mLRM) approach of Petersen et al. (2022) derived from the one-dimensional heat conservation equation for the near-surface layer of debris-covered glaciers

$$\frac{\partial T}{\partial t} = \underbrace{\frac{\partial \kappa}{\partial z}\frac{\partial T}{\partial z}}_{\text{neglected}} + \kappa \frac{\partial^2 T}{\partial z^2}, \tag{4}$$

we neglect the first derivative of κ with depth ($\frac{\partial \kappa}{\partial z}$) and stick with sLRM analysis since the variables $\frac{\partial T}{\partial z}$ and $\frac{\partial^2 T}{\partial z^2}$ strongly correlate and therefore are not suitable for mLRM analysis. In comparison to Nicholson and Benn (2013) and Petersen et al. (2022), we ensure that (1) there is no multicollinearity, (2) errors are independent, (3) residual errors are normally distributed, and (4) homoscedasticity is present aiming to exclude violations of the assumptions for linear regression by diagnostic plots (see Fig. A1, p. 18). We then only consider the valid regression models for further analysis with a significance level of $p < 0.01$.

https://doi.org/10.5194/egusphere-2024-2652
Preprint. Discussion started: 15 October 2024

Numerical model For the numerical modeling, we inverted the approach of Cicoira et al. (2019a) and solved a minimum problem between the modeled and observed temperatures. For all three neighboring sensors, we use the temperature measurement time series of the lower and upper sensors in the corresponding time window to model the temperature at the sensor in the middle. The initial condition is prescribed from the measured vertical temperature profile at the first time step of the simulation within the given time window. We perform this numerical modeling 201 times using different kappa values ranging from $0 - 20\,\mathrm{mm^2\ s^{-1}}$ with a resolution of 0.1 for each run. The temporal resolution of the model, determined by the temporal resolution of the temperature time series, is 1 day, and the vertical resolution depends on the spacing but is limited to a minimum of $0.1\,\mathrm{m}$. Comparing the numerically modeled temperature with the measured temperature at the middle sensor within the given time window, we iteratively approach the most representative value for thermal diffusivity by minimizing the RMSE (Root Mean Square Error) between the modeled and observed temperature time series at the mean sensor until the incremental difference is less than 0.1% or the mathematical minimum is reached and ensure that the normalized RMSE is < 0.05 (see Fig. A2, p. 19).

Analytical solution For the analytical solution of the heat conduction equation and the explicit calculation of the heat conduction, we followed Pogliotti et al. (2008). We assumed that annual temperature variation at any depth is sinusoidal, i.e., that conduction dominates. We then inverted the thermal diffusivity at the middle sensor of three adjacent sensors using the temperature time series from the upper and lower sensors (Horton et al., 1983; Matsuoka, 1994)

$$\kappa = \frac{\pi}{P}\left[\frac{z_1 - z_2}{\ln\left(\frac{A_1}{A_2}\right)}\right]^2, \tag{5}$$

where P (s) is the period of one complete harmonic oscillation (2π, corresponding to 365 days), A_1 and A_2 are the amplitude of the temperature waves (°C) at depths z_1 and z_2 (m), the upper and lower sensor out of the adjacent three.

3 Results and Interpretation

3.1 Murtèl-Corvatsch 2015 borehole as an illustrative example

While we apply our methods to all boreholes in the PERMOS database, we use the Murtèl-Corvatsch 2015 borehole (see 'COR_0315' in Fig. 1) as an illustrative example in Figure 2. The performance and representativeness of the derived thermal diffusivity applying the sLRM and numerical model are exemplified for a depth of $3.5\,\mathrm{m}$ and within the time window from 14 January to 14 February 2016. The statistical model fulfills all assumptions of the sLRM in this time window (see diagnostic plots in Fig. A1, p. 18) and provides an estimated thermal diffusivity of $1.12\,\mathrm{mm^2\,s^{-1}}$ with a high coefficient of determination ($R^2 = 0.86$) as well as a low p-value (< 0.001; Fig. 2a). A direct comparison between the observations on the horizontal axis with the sLRM output on the vertical axis with the model mean prediction and the 95% prediction band highlights a significant representativeness (Fig. 2b). The numerical solution provides a higher diffusivity value of $3.9\,\mathrm{mm^2\,s^{-1}}$ (yellow line in Fig. 2c) with a highly significant representativeness (Fig. 2d). Selected time windows in Figure A3 show the poor performance of

https://doi.org/10.5194/egusphere-2024-2652
Preprint. Discussion started: 15 October 2024

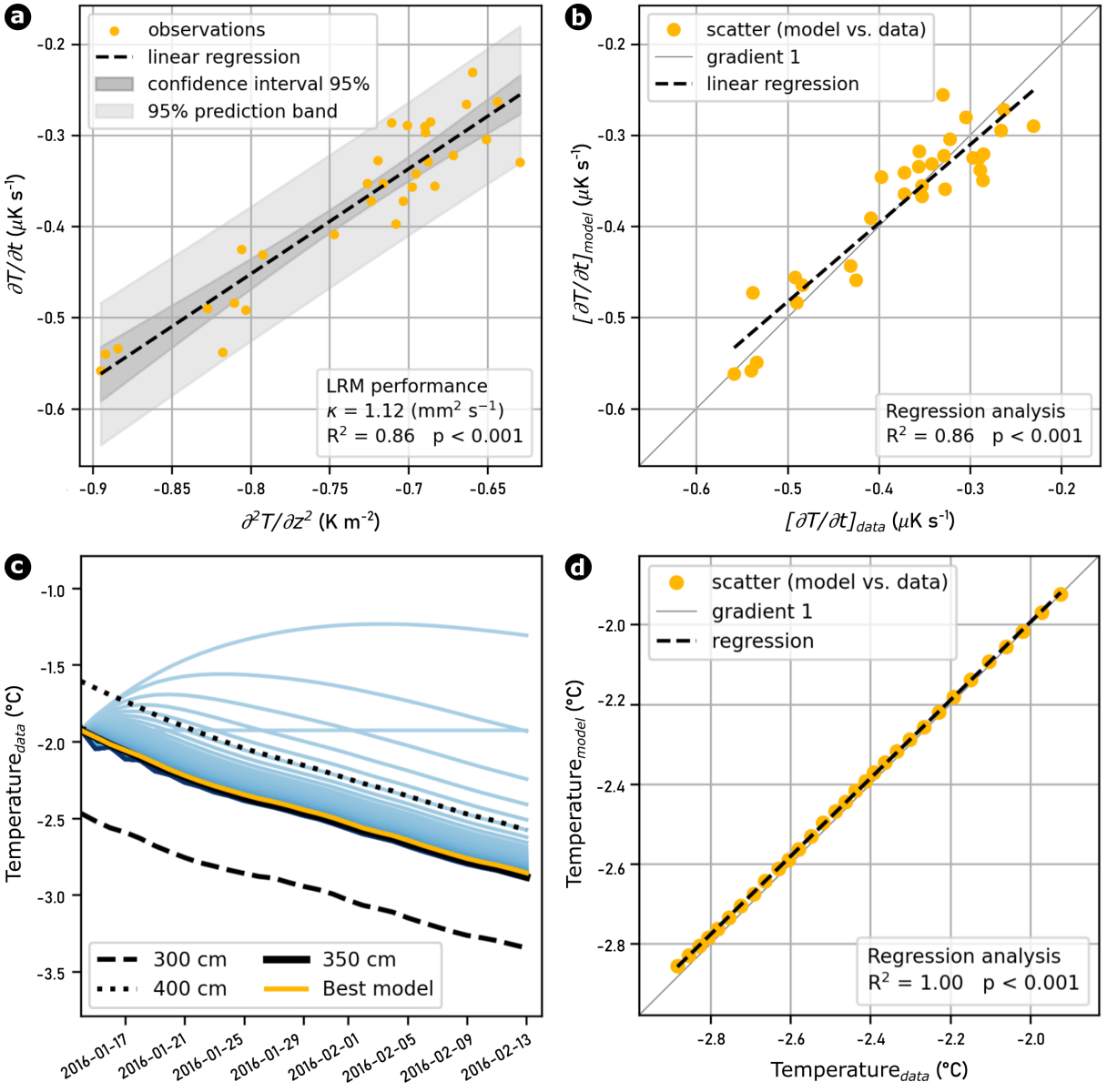

Figure 2. Modeling thermal diffusivity at the Murtèl-Corvatsch 2015 borehole. Performance and representativeness of the sLRM (a+b) and the numerical model (c+d) at 3.5 m depth and in the 1-month time window from 14 January to 14 February 2016.

the two approaches (sLRM in panels a-c and numerical model in panels d-f) when phase changes (panels a-b and d-e) or non-conductive heat flows (panels c+f) occur. This behavior results in the estimated diffusivity values being automatically omitted.

https://doi.org/10.5194/egusphere-2024-2652
Preprint. Discussion started: 15 October 2024

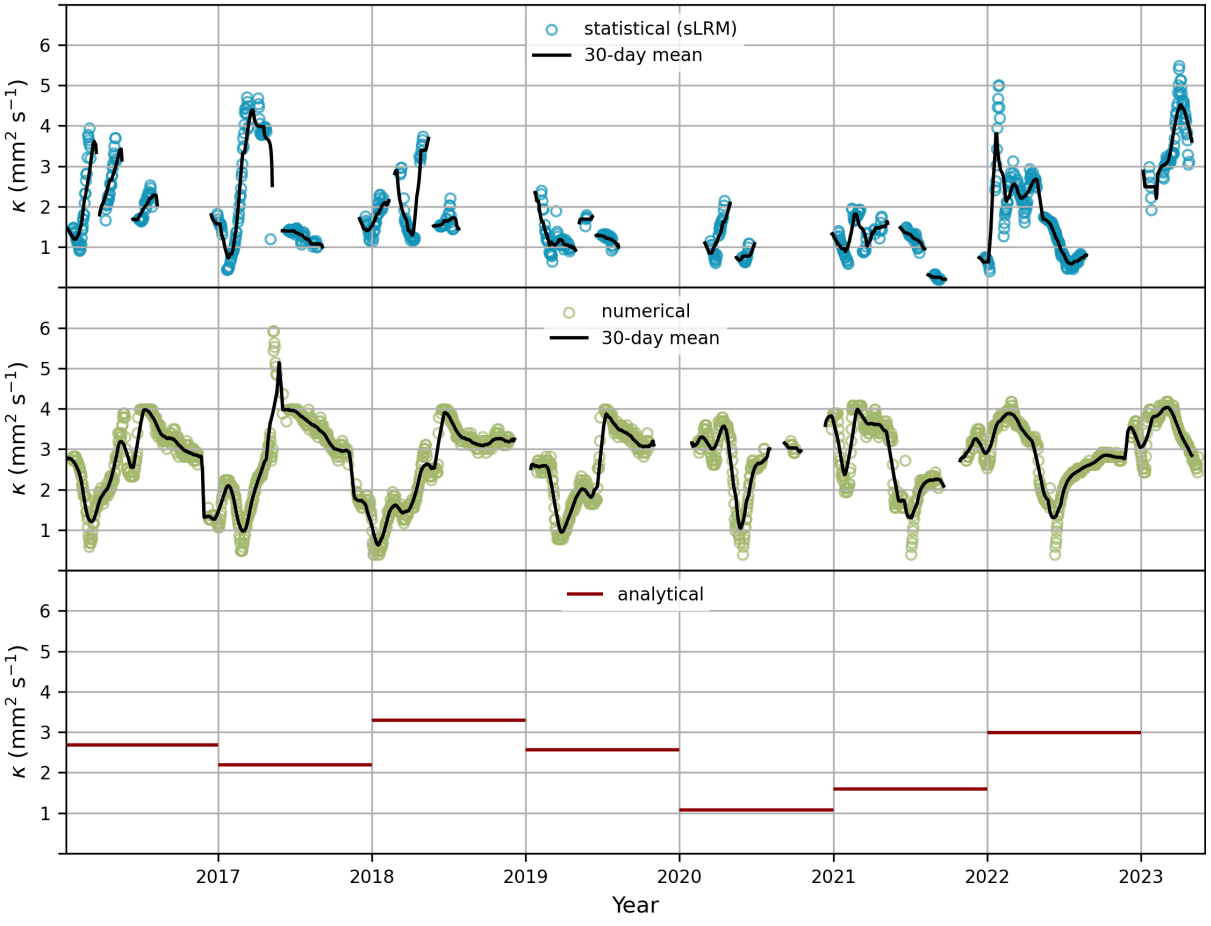

Figure 3. The multi-year time series of thermal diffusivity, derived through linear regression analysis of the heat conduction equation and inversions of numerical and analytical solutions for the Murtèl-Corvatsch 2015 borehole at 4.5 m depth. Annual means for the statistical and numerical models are not shown due to their incomplete time series.

We also observe strong temporal variations in thermal diffusivity with distinct seasonal patterns (see Fig. 3), where the pattern of sLRM and numerical model have a similar course. The thermal diffusivity could be successfully determined in considerably more time windows using numerical modeling (2134 from 2680 windows) compared to sLRM (809 from 2680 windows). Due to the deviating pattern between time series of temperature (Fig. 1c) and thermal diffusivity (Fig. 3), we assume that the cause of the fluctuations in thermal diffusivity despite sustained temperatures below 0°C is a change in the physical state of the water and thus a change in the water/ice ratio.

The thermal diffusivity values along the borehole profile for the complete time series derived by all three modeling approaches are shown in Figure 4. While the valid κ values of statistical and numerical modeling are visualized with boxplots, the median values with median absolute deviation are shown for the analytical modeling. There is great variability in thermal diffusivity in the active layer (down to a depth of around 3.5 m), while the statistical and numerical modeling shows a better

https://doi.org/10.5194/egusphere-2024-2652
Preprint. Discussion started: 15 October 2024

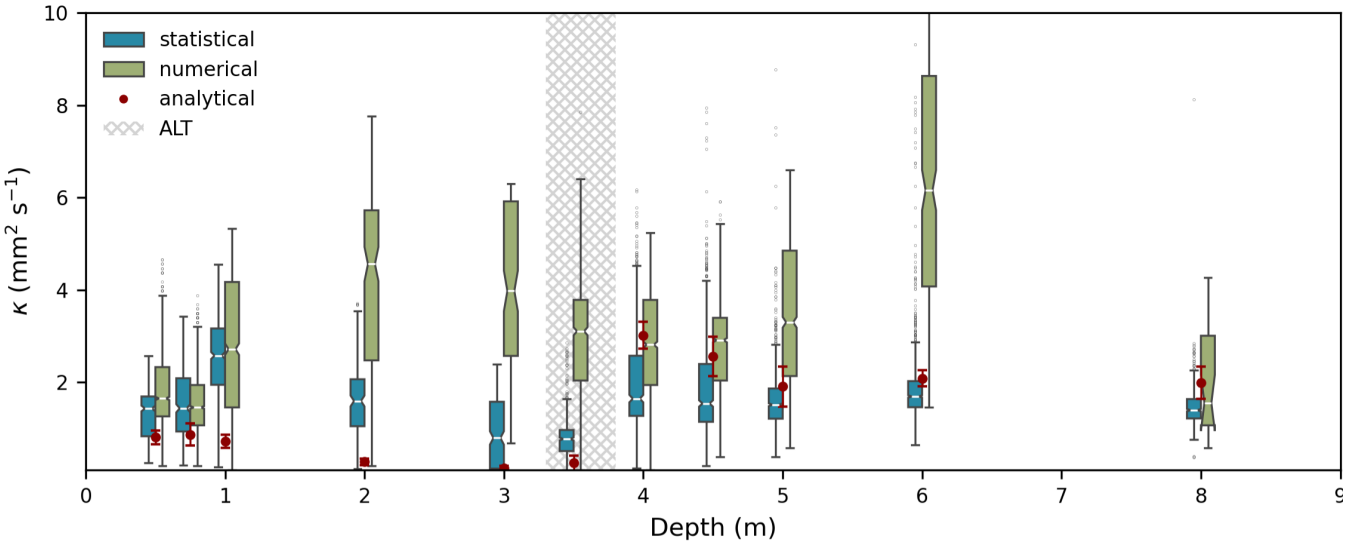

Figure 4. Thermal diffusivity values along the Murtèl-Corvatsch 2015 (COR_0315) borehole profile were derived from all three modeling approaches. The area marked in gray indicates the depth range of the permafrost table over the entire time series.

agreement in the permafrost except at a depth of 6 m. At greater depths (not visualized in Fig. 4), the modeling either fails or loses its statistical significance because the temperature amplitude becomes too small and the measurement uncertainty is of a similar order of magnitude (see discussion). The analytical modeling fits well in the upper part of the permafrost, but the deviation increases considerably with depth. While the large statistical variance in the active layer is caused by annual fluctuations in thermal diffusivity and non-conductive heat fluxes (such as heat advection due to water percolating into the ground), the deviation of the analytical solution with depth can be explained by the strong decreasing annual amplitude.

3.2 Synthetic overview of the systematic analysis

In this section, we synthesize the results of the three modeling approaches for all the PERMOS temperature boreholes, categorized according to the landform documented in the PERMOS metadata (PERMOS, 2024). Distinguishing between the near-surface layer (active layer or freeze/thaw layer) and the area below (permafrost or year-round unfrozen zones), the valid κ values of statistical analysis and numerical modeling are visualized with boxplots for all boreholes in Figure 5a+b, complemented by the median values with the mean absolute deviation of the analytical modeling. Value ranges of the medians and the 5- to 95-percentile ranges are given below for each landform and each modeling approach. While numerical modeling exhibits larger variances and inter-quantile ranges (IQR) than statistical modeling in the permafrost zone, we observe an opposite but weaker pattern in the active layer. Furthermore, apparent differences and strong scattering can be seen in the 5- to 95-percentile ranges across all landforms and modeling approaches.

Across all modeling approaches and landforms, these results indicate typical thermal diffusivity values in the 25- to 75-percentile range of $1.1 - 3.3\,\mathrm{mm^2\ s^{-1}}$ for permafrost and $0.8 - 2.4\,\mathrm{mm^2\ s^{-1}}$ for the overlying active layer. There is no overall

https://doi.org/10.5194/egusphere-2024-2652
Preprint. Discussion started: 15 October 2024

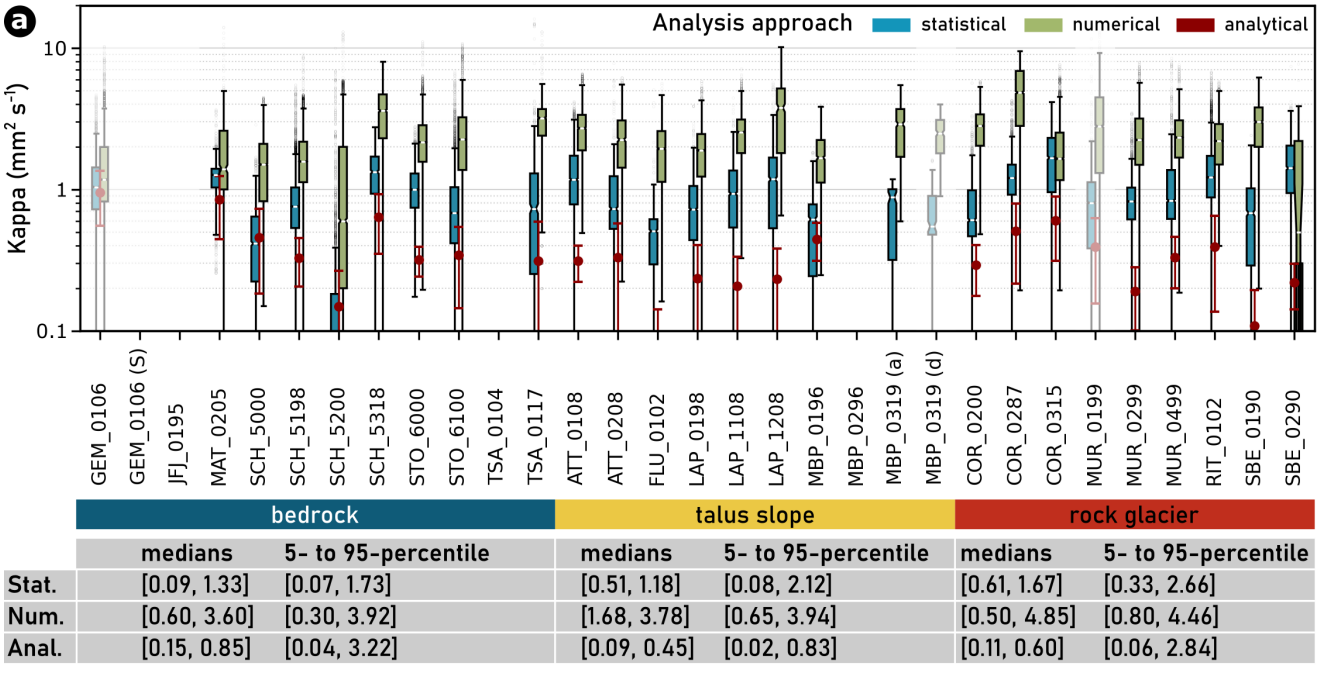

	bedrock		talus slope		rock glacier	
	medians	5- to 95-percentile	medians	5- to 95-percentile	medians	5- to 95-percentile
Stat.	[0.09, 1.33]	[0.07, 1.73]	[0.51, 1.18]	[0.08, 2.12]	[0.61, 1.67]	[0.33, 2.66]
Num.	[0.60, 3.60]	[0.30, 3.92]	[1.68, 3.78]	[0.65, 3.94]	[0.50, 4.85]	[0.80, 4.46]
Anal.	[0.15, 0.85]	[0.04, 3.22]	[0.09, 0.45]	[0.02, 0.83]	[0.11, 0.60]	[0.06, 2.84]

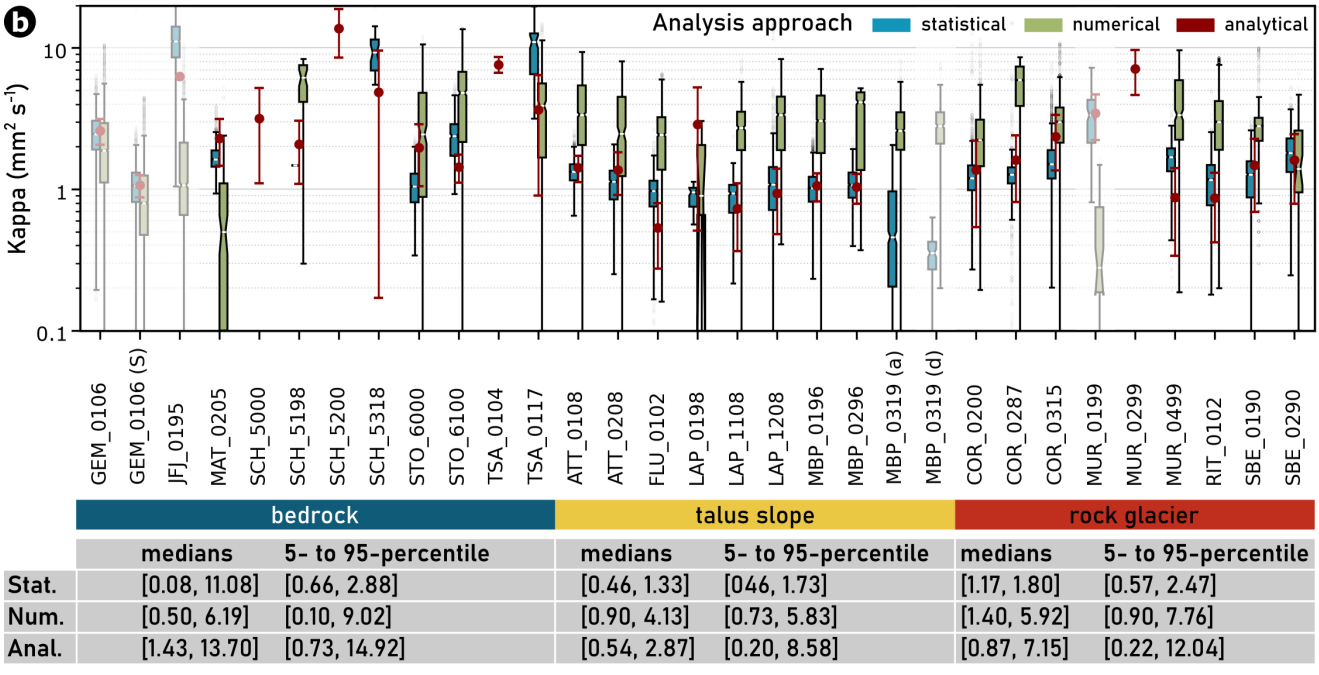

	bedrock		talus slope		rock glacier	
	medians	5- to 95-percentile	medians	5- to 95-percentile	medians	5- to 95-percentile
Stat.	[0.08, 11.08]	[0.66, 2.88]	[0.46, 1.33]	[046, 1.73]	[1.17, 1.80]	[0.57, 2.47]
Num.	[0.50, 6.19]	[0.10, 9.02]	[0.90, 4.13]	[0.73, 5.83]	[1.40, 5.92]	[0.90, 7.76]
Anal.	[1.43, 13.70]	[0.73, 14.92]	[0.54, 2.87]	[0.20, 8.58]	[0.87, 7.15]	[0.22, 12.04]

Figure 5. Modeled thermal diffusivity sorted by landform for the active layer (a) and the permafrost body (b). While all PERMOS boreholes are illustrated in the boxplot panels, boreholes that do not directly measure permafrost (GEM_0106, GEM_0106 (S), MUR_0199) and another borehole due to its exceptional orientation with lateral heat conduction (JFJ_0195) are excluded from the statistical description.

https://doi.org/10.5194/egusphere-2024-2652
Preprint. Discussion started: 15 October 2024

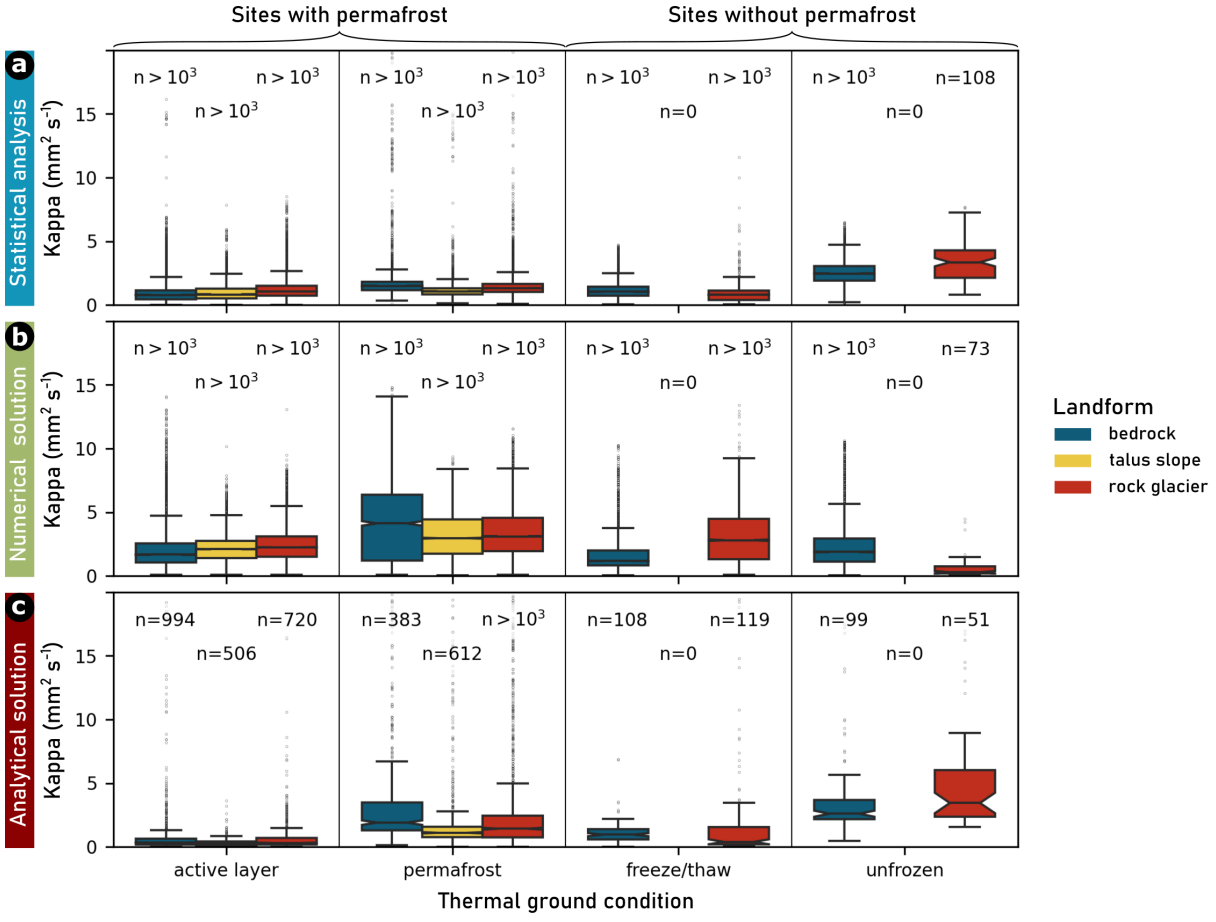

Figure 6. Thermal diffusivity values of all PERMOS boreholes but JFJ_0195 grouped by ground conditions and sorted by landform derived by (a) sLRM analysis, (b) numerical modeling, and (c) analytical solution of the heat conduction equation.

valid pattern of thermal diffusivity as a function of landform or thermal ground conditions (see Fig. 6), although landforms differ greatly in their composition. Considering only the thermal ground condition active layer and permafrost (sites with permafrost, see left part of Fig. 6), there is a small but significant difference (Mann-Whitney-U-Test $p < 0.01$) in thermal diffusivity between the landforms for all three approaches. Looking at the statistical analysis and numerical modeling, the ascending order of landforms by thermal diffusivity is bedrock - talus slope - rock glacier in the permafrost and rock glacier - talus slope - bedrock in the active layer. In comparison, distinctly different values were only found in year-round unfrozen zones at locations without permafrost. The difference between bedrock (only borehole GEM_0106) and rock glaciers (only borehole MUR_0199) in this thermal group is also evident, but also with remarkable variances and inter-quantile ranges most likely due to a small number of considered windows.

https://doi.org/10.5194/egusphere-2024-2652
Preprint. Discussion started: 15 October 2024

4 Discussion

4.1 Approaches to empirically quantify thermal diffusivity

This study presents a systematic analysis of thermal diffusivity in mountain permafrost, applying three independent modeling approaches, and thereby provides for the first time a well-constrained range of empirically derived thermal diffusivity values of mountain permafrost (25- to 75-percentile range: $1.1 - 3.3\,\mathrm{mm^2\ s^{-1}}$). For all 29 PERMOS temperature boreholes, we successfully quantify the thermal diffusivity at different depths along the profile and over time using simple linear regression analysis (sLRM), numerical modeling, and analytical solution of the heat conduction equation. Overall, thermal diffusivity variability decreases with depth unless there is a non-conductive heat flux. While the ground temperature, which is characterized by seasonal fluctuations and phase change resulting in varying water/ice ratios, and the associated thermal diffusivity in the active layer vary strongly, the signal tends to approximate thermal conductivity conditions in the permafrost body, with less scatter but still with strong seasonal evolution (see Fig. 7a+b). The temperature variations become too small below a certain threshold depth, typically around $8 - 15\,\mathrm{m}$, and the analysis loses its statistical significance.

All three applied modeling approaches assume a conductive heat exchange along the temperature profile and homogeneous material properties between the three neighboring sensors. For the 1D heat conduction equation, the sLRM is relatively straightforward to implement and requires less computational resources than the numerical solutions. The analytical model is also computationally efficient and is particularly useful for quick estimations. Still, it relies on simplifying assumptions to derive closed-form solutions of the mathematical equation describing the diffusivity. In nature, conductive heat exchange is highly variable and sometimes superimposed by other heat transfer processes. The validity and the quality of the results of all three modeling approaches are determined by (i) the occurrence of non-conductive processes, (ii) measurement constraints such as the accuracy of the temperature data or the depth of the thermistors, and (iii) analysis parameters such as the window size of the points considered.

The sLRM is the most applicable modeling approach for empirically quantifying thermal diffusivity in cold regions where phase changes are suspected (Williams and Smith, 1991; Nicholson and Benn, 2013), since the temperature rate ($\frac{\partial T}{\partial z}$) is essentially zero and therefore no valid regression analysis with temperature Laplacian ($\frac{\partial^2 T}{\partial z^2}$) is possible. Despite specific differences between the outputs of the three approaches, the range of thermal diffusivity values derived with sLRM could successfully be validated with the numerical modeling and the analytical solution (see Fig. 5 or additional validation based on thermal diffusivity values grouped by thermal ground conditions and sorted by landform is given in Fig. 6). This validation demonstrates the strong performance of the simple Linear Regression Model (sLRM), as we observed a consistent agreement between the derived diffusivity values, with deviations typically limited to a factor of 2. However, the sLRM additionally depends on the first derivative with respect to time (temperature rate) and the second derivative with respect to depth (temperature Laplacian). These become smaller and smaller with depth, whereby the signal decreases or is even lost with increasing depth. Therefore, the assumptions for the linear regression's validity are checked for each application, and the results are discarded if violated. Nevertheless, the sLRM also fails if not enough measuring points are characterized by pure conductive heat exchange. How-

https://doi.org/10.5194/egusphere-2024-2652
Preprint. Discussion started: 15 October 2024

ever, this does not necessarily mean that advective heat flux is present or even dominates, as phase change also influences the temperature profiles and, thus, the model performance.

Overall, the thermal diffusivity time series derived from numerical modeling tends to be more complete but needs to be interpreted carefully when the temperature amplitude is getting small and the derived diffusivity values change rapidly or scatter. While the sLRM approach dispenses with windows with outliers, as the regression assumptions are violated, the numerical modeling can principally result in slightly too high values in isolated time windows with short-term advective heat flows, as the numerical solution attempts to approximate the non-conductive temperature curve with conductive heat transport - Figure A3 shows that such time windows are usually discarded. Nonetheless, we recommend considering the results of the three approaches in combination and, if applicable, considering time windows and depths with matching values for further analyses.

4.2 On the potential to identify non-conductive heat fluxes

The occurrence of permafrost strongly influences the hydraulic properties in a rock mass (Pogrebiskiy and Chernyshev, 1977; Haeberli et al., 1997). The hydraulic permeability, for example, is much lower in rock masses with frozen and ice-filled fractures than in unfrozen ones (Pogrebiskiy and Chernyshev, 1977), where ice plugs can prevent water percolation to greater depths, leading to lateral/surface runoff (Hasler et al., 2011). Rock masses at several degrees below $0°C$ are sensitive to percolating water (Stähli et al., 1996; Boike et al., 1998; Scherler et al., 2010). For instance, rapid water percolation through wide fractures results in minimal heat exchange along the flowing path within the unsaturated zone and thereby increases the efficiency of the advective heat transfer to the ice level at depth in fractures (Hasler et al., 2011), similar to observations in the talus (Rist and Phillips, 2005). This effect leads to a heat transport shortcut between the surface (or atmosphere) and the plugging ice level. Non-conductive heat fluxes, such as heat advection by deep water infiltration, are of particular interest as they can lead to accelerated warming of the ground, which can cause several problems, for example, inducing deep-seated slope instabilities or complicating construction work.

There are only a few observations of water fluxes in permafrost. Still, these can change rapidly over time due to the thickening of the active layer, warming of the permafrost, melting of the ground ice, formation of talik, and related modification in permeability (Zenklusen Mutter and Phillips, 2012; Haberkorn et al., 2021; Smith et al., 2022). So far, efforts have been made to detect non-conductive heat fluxes in mountain permafrost, aiming to determine the timing, depth, and duration. Among others, anomalies in spectral analysis of temperature time series (Hinkel and Outcalt, 1993; Hasler, 2011), simulations with different heat sources and sinks (Luethi et al., 2017), temperature contour plots showing flags in the $0°C$ isotherm (e.g., Luethi and Phillips, 2016), or outliers and jumps in the temperature time series (Phillips et al., 2016; Offer et al., 2024) appear to be promising indicators for non-conductive heat fluxes. However, there are only qualitative indications based on manual selection.

The time-depths-thermal diffusivity plot and a depth profile with thermal diffusivity boxplots for the top $15\,m$ of the Murtèl-Corvatsch 2015 borehole are shown in Figure 7a+b indicating substantial variability over time and with depth. Although thermal diffusivity changes in space and time, we can indirectly identify short-term periods with non-conductive processes: First, we combine observed temperature rates ($\partial T/\partial t$, dots colored by month) with the 95% prediction band (gray area) of the sLRM over time (see Fig. 7c) and across the temperature Laplacian (see Fig. 7e). Then, we select periods with observations

https://doi.org/10.5194/egusphere-2024-2652
Preprint. Discussion started: 15 October 2024

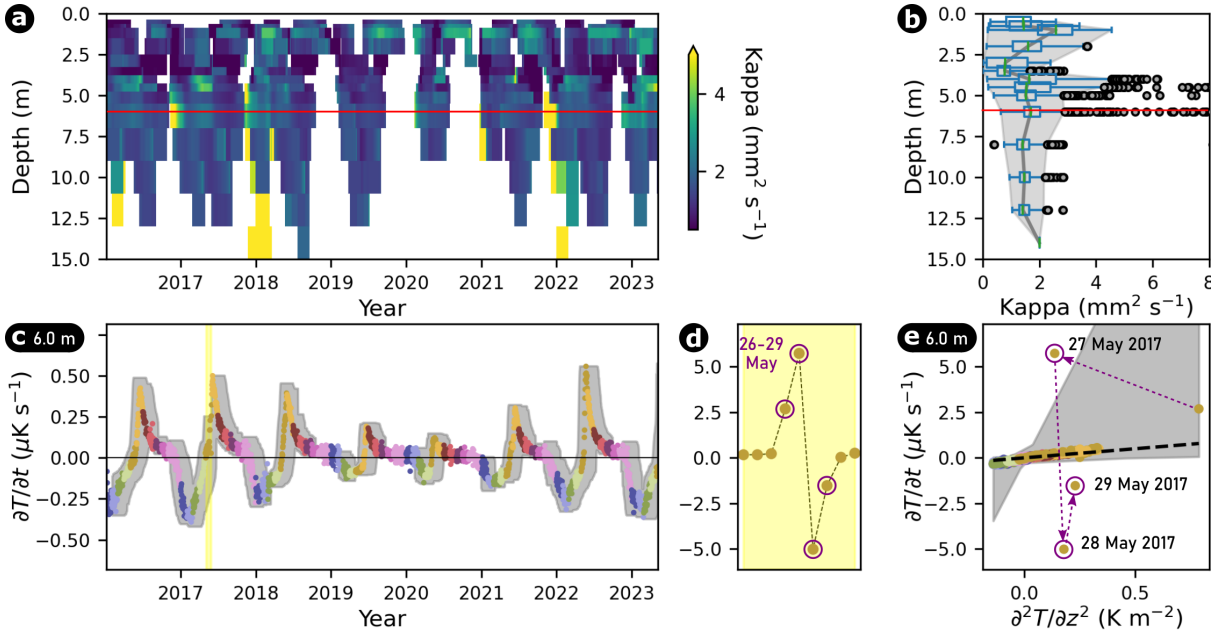

Figure 7. Thermal diffusivity values, derived through linear regression analysis of the heat conduction equation for the Murtèl-Corvatsch 2015 borehole. For the top 15 m, (a) shows the time-depths-thermal diffusivity plot and (b) a profile with boxplots of all diffusivity values for each depth instrumented with a thermistor. (c) The temperature rate at 6 m depth for the entire time series (yellow area from 23-31 May is shown in (d) with different y-scale) and (e) a temperature-rate/temperature-Laplacian scatter combining observations (colored by month) and the 95% prediction bands of all valid linear regression models (a gray area with large scattering due to seasonal evolution) that can be used to identify outliers and, thus, the occurrence of non-conductive processes.

that show a significant deviation from the $\partial T/\partial t$ zero line to exclude periods determined by phase changes. Finally, we isolate observations that lie outside the model prediction band, such as 27-29 May 2017 (see Fig. 7d+e), and interpret them as temporary periods governed by non-conductive processes.

We consider and analyze several sensor depths together to gain more confidence in this approach and rule out measurement inaccuracies and errors. Figure 8, showing the temperature rates and the 95% prediction ranges of all valid linear regression models for different depths, is further evidence that non-conductive heat transport processes characterize the period from 26 to 29 May 2017. We identified the anomalies, most likely caused by snowmelt from the surface, simultaneously at four different depths from 4 to 6 m but not at the underlying thermistor at 8 m depth. A technical problem can be ruled out, as only certain depths show such anomalies for a short period of time. These identified non-conductive heat flow periods agree well with recently published studies on the presence and influence of water at this site (e.g., Cicoira et al., 2019a; Amschwand et al., 2023).

https://doi.org/10.5194/egusphere-2024-2652
Preprint. Discussion started: 15 October 2024

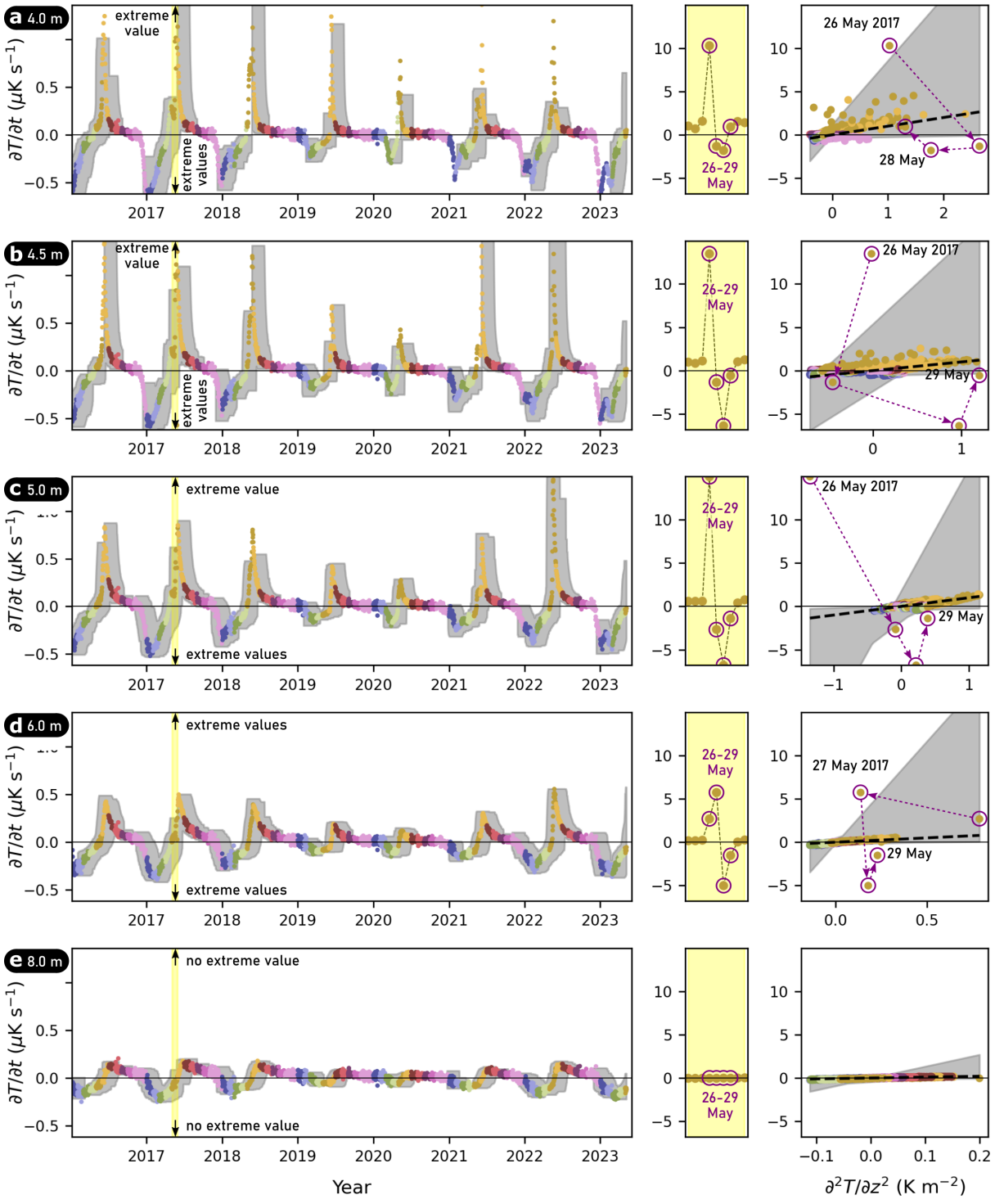

Figure 8. Temperature rates for the entire time series with zoom on 23-31 May (yellow area) and a temperature-rate/temperature-Laplacian scatter with observations (colored by month) and the prediction ranges of all valid linear regression models for different depths along the Murtèl-Corvatsch 2015 (COR_0315) borehole.

https://doi.org/10.5194/egusphere-2024-2652
Preprint. Discussion started: 15 October 2024

4.3 Thermo-mechanical response to climate change

Even for studies without boreholes, the well-constrained range of thermal diffusivity values and their annual course directly benefit a variety of models, including those for ground temperature distributions, either as input parameters or for validation. However, no general seasonal pattern for different sites and depths could be identified. If a borehole with temperature sensors exists, regardless of the ground material, the three proposed approaches to estimating diffusive heat exchange can principally be applied providing site- and depth-specific time-series of thermal diffusivity. As thermal diffusivity depends on the thermal material properties, the site-specific thermal diffusivity time series at different depths can either be used for energy balance models by coupling solar radiation measurements with heat conduction or to get valuable insights into the temporal evolution of the thermal regime. This evolution can potentially be linked to changes in water content or the physical state of water and the related water/ice ratio. Therefore, site-specific seasonal patterns and possible shifts or alterations in shape can be a valuable addition to other prospecting methods to track changes in ground composition/properties.

The latter is a prerequisite for reliable thermo-mechanical stability analysis and modeling in a changing climate as many mechanical properties and processes depend on temperature, the increasing occurrence of liquid water due to phase change of present ice and/or the formation of ice. Cohesive rock bridges can for example be destroyed by reducing compressive and tensile strength during the thawing of saturated rock (Mellor, 1973) or reaching the fatigue life through periodic loading of discontinuities due to thermo-mechanical effects (Jia et al., 2015; Murton et al., 2016). Warming also affects the rock-ice mechanics of permafrost rock slopes (Krautblatter et al., 2013) and indirectly also controls the cohesion and friction in ice-filled discontinuities leading to a decrease in shear resistance (Mamot et al., 2018). The frequently observed exposure of ice and outflow of water in the scarps after rock slope failures support the theory of an increase in rock slope destabilization due to changing thermal and hydrologic conditions in mountain permafrost; for instance, observed at Kolka-Karmadon (Huggel et al., 2005), Mt Steller (Huggel, 2009), Matterhorn (Weber et al., 2019), or Piz Kesch (Phillips et al., 2017).

5 Conclusions

The systematic analysis of the PERMOS borehole temperature data, with three independent models, allows us to derive a well-constrained range for the thermal diffusivity in mountain permafrost with different landforms such as bedrock, talus slopes, and rock glaciers. These values and their annual course directly benefit a variety of models, among others, for ground temperature distributions or energy balance estimates, even in the absence of boreholes either for calibration or validation. In addition to such direct applications, for locations with temperature boreholes, we have established an indirect approach to empirically identify and investigate non-conductive processes driven by thawing and/or water advection by isolating spatial and temporal anomalies in thermal diffusivity. Further development of this approach, considering seasonal variability (see Fig. 7a), will allow us to quantify the non-conductive heat flux. This study thereby represents the basis for investigating mountain permafrost slopes' thermal and mechanical behavior. For example, the site-specific ratio of available energy dissipated through turbulent fluxes can be estimated by combining heat conduction, which can be calculated based on thermal diffusivity and borehole temperature data, with net radiation measurements. Finally, the three approaches to model diffusive heat exchange

https://doi.org/10.5194/egusphere-2024-2652
Preprint. Discussion started: 15 October 2024

presented and the Python module (Weber, 2024) developed can be applied to any temperature profile in the ground, regardless of the material.

Code and data availability. The processed and quality-controlled borehole temperature data set used for this study originates from the Swiss Permafrost Monitoring Network (PERMOS, 2024). The analysis code with the implementation of the three modeling approaches is written in Python 3 and will be published on Zenodo before the final publication of this manuscript (Weber, 2024).

Appendix A: Visualization of the methodological approach

This appendix provides (i) examples of a diagnostic diagram to check the assumptions for linear regression analysis (Fig. A1), (ii) the most representative thermal diffusivity value for numerical modeling (Fig. A2), and (iii) the performance of statistical analysis and numerical modeling when phase changes or non-conductive heat fluxes occur (Fig. A3).

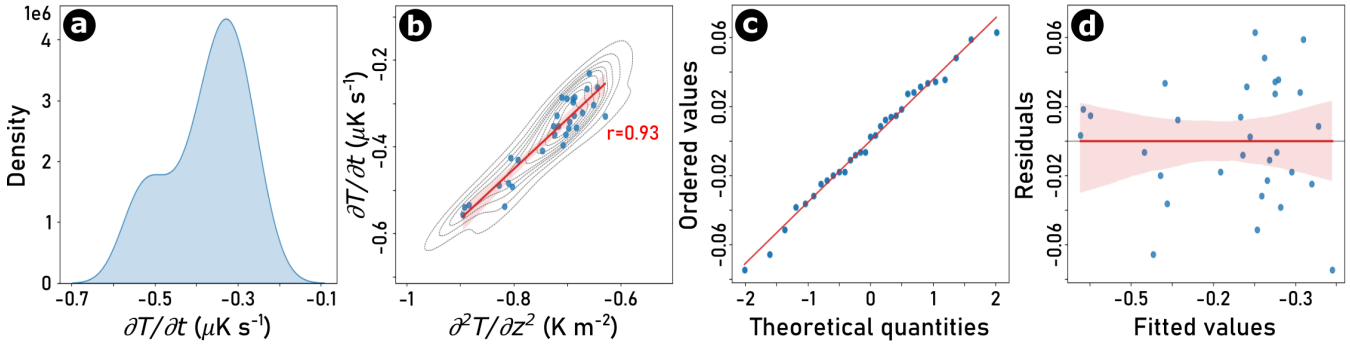

Figure A1. Diagnostic plots to prove the assumptions for linear regression analysis between IV (independent variable) and DV (dependent variable) – as an illustrative example the Murtèl-Corvatsch 2015 (COR_0315) borehole at a depth of 3.5 m and within the time window from 14 January to 14 February 2016. (a) Proof that predictors are distributed normally. (b) Proof the linear relation between the DV and the IV. (c) Proof the normality of the residual errors to confirm that both datasets (DV and IV) have a common distribution: All point of quantiles should lie on or close to straight line with a gradient of 1. (d) Proof the homoscedasticity (or equal variance) of residuals: Spread of the residuals from the linear regression model should be homogeneous or equal spaces.

Author contributions. SW and AC developed the study's concept together. SW implemented the three modeling approaches, performed the analysis, and made the figures in Python 3. SW prepared the manuscript with revision and final approval from AC.

Competing interests. The authors declare no competing interests.

https://doi.org/10.5194/egusphere-2024-2652
Preprint. Discussion started: 15 October 2024

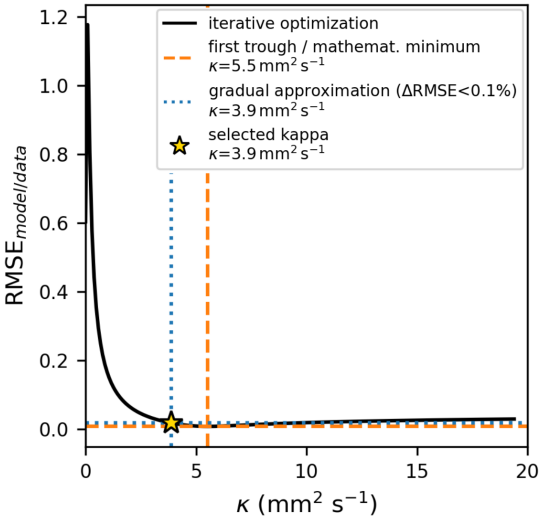

Figure A2. Iterative approximation to the most representative value for the thermal diffusivity by minimizing the RMSE (Root Mean Square Error; solid black line) between the modeled and the observed temperature time series until the incremental difference is less than 0.1% (dotted blue line) or the mathematical minimum (dashed orange line) is reached – as an illustrative example the Murtèl-Corvatsch 2015 (COR_0315) borehole at a depth of 3.5 m and within the time window from 14 January to 14 February 2016.

Acknowledgements. The authors would like to thank Andreas Vieli and Vanessa Wirz for their exploratory preliminary work, and Andreas, in particular, for his thermal diffusivity model in Matlab. Our thanks also go to our colleagues at the WSL Institute for Snow and Avalanche Research SLF Davos, namely Alexander Bast for his valuable advice on the statistical analysis, Marcia Phillips for her constructive comments, and Jeannette Nötzli for her additional explanation and insight into the PERMOS (meta-) data. The borehole temperature data (PERMOS, 2024) used in this study originate from the Swiss Permafrost Monitoring Network (PERMOS), the PERMOS office and its six partner institutions ETH Zurich (ETHZ), the Universities of Fribourg (UniFR), Lausanne (UniL) and Zurich (UZH), the University of Applied Sciences of Southern Switzerland (SUPSI) and the WSL Institute for Snow and Avalanche Research SLF Davos (SLF) – supported by MeteoSwiss (as part of GCOS Switzerland), BAFU and SCNAT.

https://doi.org/10.5194/egusphere-2024-2652
Preprint. Discussion started: 15 October 2024

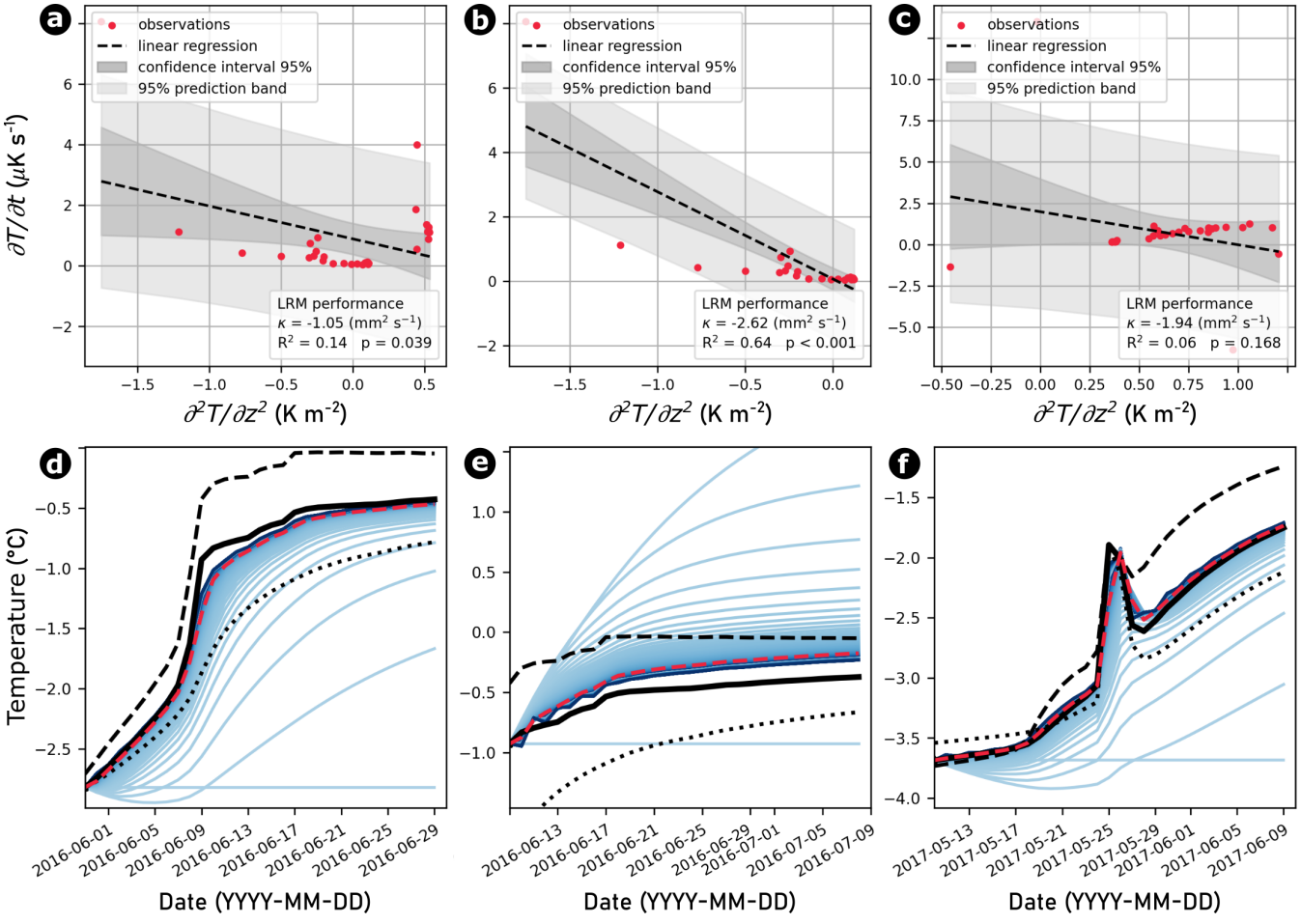

Figure A3. Exemplary 1-month time windows at the Murtèl-Corvatsch 2015 borehole show that the sLRM (a-c) and the numerical model (d-f) approaches fail during periods characterized by phase change (a-b and d-e) or non-conductive heat fluxes (c and f).

References

Amschwand, D., Scherler, M., Hoelzle, M., Krummenacher, B., Haberkorn, A., Kienholz, C., and Gubler, H.: Surface heat fluxes at coarse-blocky Murtèl rock glacier (Engadine, eastern Swiss Alps), EGUsphere, 2023, 1–56, https://doi.org/10.5194/egusphere-2023-2109, 2023.

Bast, A., Kenner, R., and Phillips, M.: Short-term cooling, drying and deceleration of an ice-rich rock glacier, EGUsphere, pp. 1–26, https://doi.org/10.5194/egusphere-2024-269, 2024.

Biskaborn, B. K., Smith, S. L., Noetzli, J., Matthes, H., Vieira, G., Streletskiy, D. A., Schoeneich, P., Romanovsky, V. E., Lewkowicz, A. G., Abramov, A., Allard, M., Boike, J., Cable, W. L., Christiansen, H. H., Delaloye, R., Diekmann, B., Drozdov, D., EtzelmÃ¼ller, B., Grosse, G., Guglielmin, M., Ingeman-Nielsen, T., Isaksen, K., Ishikawa, M., Johansson, M., Johannsson, H., Joo, A., Kaverin, D., Kholodov, A., Konstantinov, P., KrÃ¶ger, T., Lambiel, C., Lanckman, J.-P., Luo, D., Malkova, G., Meiklejohn, I., Moskalenko, N., Oliva, M., Phillips,

https://doi.org/10.5194/egusphere-2024-2652
Preprint. Discussion started: 15 October 2024

M., Ramos, M., Sannel, A. B. K., Sergeev, D., Seybold, C., Skryabin, P., Vasiliev, A., Wu, Q., Yoshikawa, K., Zheleznyak, M., and Lantuit, H.: Permafrost is warming at a global scale, Nature Communications, 10, 264, https://doi.org/10.1038/s41467-018-08240-4, 2019.

Blackwell, D. D. and Steele, J. L.: Heat flow and geothermal potential of Kansas, Bulletin (Kansas Geological Survey), pp. 267–295, https://journals.ku.edu/kgsbulletin/article/view/20508, 1989.

Boike, J., Roth, K., and Overduin, P. P.: Thermal and hydrologic dynamics of the active layer at a continuous permafrost site (Taymyr Peninsula, Siberia), Water Resources Research, 34, 355–363, https://doi.org/10.1029/97WR03498, 1998.

Bonnaventure, P. P. and Lamoureux, S. F.: The active layer: A conceptual review of monitoring, modelling techniques and changes in a warming climate, Progress in Physical Geography: Earth and Environment, 37, 352–376, https://doi.org/10.1177/0309133313478314, 2013.

Carslaw, H. S. and Jaeger, J. C.: Conduction of heat in solids, Oxford Science Publica-tions. Clarendon Press, 2, 1959.

Cicoira, A., Beutel, J., Faillettaz, J., Gärtner-Roer, I., and Vieli, A.: Resolving the influence of temperature forcing through heat conduction on rock glacier dynamics: a numerical modelling approach, The Cryosphere, 13, 927–942, https://doi.org/10.5194/tc-13-927-2019, 2019a.

Cicoira, A., Beutel, J., Faillettaz, J., and Vieli, A.: Water controls the seasonal rhythm of rock glacier flow, Earth and Planetary Science Letters, 528, 115 844, https://doi.org/10.1016/j.epsl.2019.115844, 2019b.

Cicoira, A., Marcer, M., Gärtner-Roer, I., Bodin, X., Arenson, L. U., and Vieli, A.: A general theory of rock glacier creep based on in-situ and remote sensing observations, Permafrost and Periglacial Processes, 32, 139–153, https://doi.org/10.1002/ppp.2090, 2021.

Clauser, C. and Huenges, E.: Thermal Conductivity of Rocks and Minerals, in: Rock Physics & Phase Relations, pp. 105–126, American Geophysical Union (AGU), https://onlinelibrary.wiley.com/doi/abs/10.1029/RF003p0105, 1995.

Conway, H. and Rasmussen, L.: Summer temperature profiles within supraglacial debris on Khumbu Glacier, Nepal, in: Debris-Covered Glaciers, IAHS Publication, vol. 264, Seattle, Washington, USA, 2000.

Draebing, D. and Krautblatter, M.: P-wave velocity changes in freezing hard low-porosity rocks: A laboratory-based time-average model, The Cryosphere, 6, 1163–1174, https://doi.org/10.5194/tc-6-1163-2012, 2012.

Fourier, J.-B.-J.: Théorie analytique de la chaleur, Didot, 1822.

Haberkorn, A., Kenner, R., Noetzli, J., and Phillips, M.: Changes in Ground Temperature and Dynamics in Mountain Permafrost in the Swiss Alps, Frontiers in Earth Science, 9, https://www.frontiersin.org/articles/10.3389/feart.2021.626686, 2021.

Haeberli, W., Wegmann, M., and Mühll, D. V.: Slope stability problems related to glacier shrinkage and permafrost degradation in the Alps, Eclogae Geologicae Helvetiae, 90, 407–414, https://doi.org/10.5169/seals-168172, 1997.

Haeberli, W., Hallet, B., Arenson, L., Elconin, R., Humlum, O., Kääb, A., Kaufmann, V., Ladanyi, B., Matsuoka, N., Springman, S., and Vonder Mühll, D.: Permafrost creep and rock glacier dynamics, Permafrost and Periglacial Process., 17, 189–214, https://doi.org/0.1002/ppp.561, 2006.

Haigh, S.: Thermal conductivity of sands, Géotechnique, 62, 617–625, https://doi.org/10.1680/geot.11.P.043, 2012.

Hanson, S. and Hoelzle, M.: The thermal regime of the active layer at the Murtèl rock glacier based on data from 2002, Permafrost and Periglacial Processes, 15, 273–282, https://doi.org/10.1002/ppp.499, 2004.

Hasler, A.: Thermal conditions and kinematics of steep bedrock permafrost, PhD Thesis, University of Zurich, 2011.

Hasler, A., Gruber, S., Font, M., and Dubois, A.: Advective heat transport in frozen rock clefts: Conceptual model, laboratory experiments and numerical simulation, Permafrost and Periglacial Process., 22, 378–389, https://doi.org/10.1002/ ppp.737, 2011.

Hinkel, K. M. and Outcalt, S. I.: Detection of nonconductive heat transport in soils using spectral analysis, Water Resources Research, 29, 1017–1023, https://doi.org/10.1029/92WR02596, 1993.

https://doi.org/10.5194/egusphere-2024-2652
Preprint. Discussion started: 15 October 2024

Horton, R., Wierenga, P. J., and Nielsen, D. R.: Evaluation of Methods for Determining the Apparent Thermal Diffusivity of Soil Near the Surface, Soil Science Society of America Journal, 47, 25–32, https://doi.org/10.2136/sssaj1983.03615995004700010005x, 1983.

Huggel, C.: Recent extreme slope failures in glacial environments: effects of thermal perturbation, Quaternary Science Reviews, 28, 1119–1130, https://doi.org/10.1016/j.quascirev.2008.06.007, 2009.

Huggel, C., Zgraggen-Oswald, S., Haeberli, W., Kääb, A., Polkvoj, A., Galushkin, I., and Evans, S. G.: The 2002 rock/ice avalanche at Kolka/Karmadon, Russian Caucasus: Assessment of extraordinary avalanche formation and mobility, and application of QuickBird satellite imagery, Natural Hazards and Earth System Sciences, 5, 173–187, https://doi.org/10.5194/nhess-5-173-2005, 2005.

IPCC: The Ocean and Cryosphere in a Changing Climate: Special Report of the Intergovernmental Panel on Climate Change, Cambridge University Press, Cambridge, https://www.cambridge.org/core/books/ocean-and-cryosphere-in-a-changing-climate/A05E6C9F8638FA7CE1748DE2EB7B491B, 2022.

Jia, G. S., Tao, Z. Y., Meng, X. Z., Ma, C. F., Chai, J. C., and Jin, L. W.: Review of effective thermal conductivity models of rock-soil for geothermal energy applications, Geothermics, 77, 1–11, https://doi.org/10.1016/j.geothermics.2018.08.001, 2019.

Jia, H., Xiang, W., and Krautblatter, M.: Quantifying rock fatigue and decreasing compressive and tensile strength after repeated freeze-thaw cycles, Permafrost and Periglacial Process., 26, 368–377, https://doi.org/10.1002/ppp.1857, 2015.

Kenner, R., Pruessner, L., Beutel, J., Limpach, P., and Phillips, M.: How rock glacier hydrology, deformation velocities and ground temperatures interact: Examples from the Swiss Alps, Permafrost and Periglacial Processes, 31, 3–14, https://doi.org/10.1002/ppp.2023, 2020.

Krautblatter, M. and Hauck, C.: Electrical resistivity tomography monitoring of permafrost in solid rock walls, Journal of Geophysical Research: Earth Surface, 112, F02S20, https://doi.org/10.1029/2006JF000546, 2007.

Krautblatter, M., Funk, D., and Günzel, F.: Why permafrost rocks become unstable: A rock-ice-mechanical model in time and space, Earth Surf. Process. Landf., 38, 876–887, https://doi.org/10.1002/esp.3374, 2013.

Labus, M. and Labus, K.: Thermal conductivity and diffusivity of fine-grained sedimentary rocks, Journal of Thermal Analysis and Calorimetry, 132, 1669–1676, https://doi.org/10.1007/s10973-018-7090-5, 2018.

Luethi, R. and Phillips, M.: Challenges and solutions for long-term permafrost borehole temperature monitoring and data interpretation, Geographica Helvetica, 71, 121–131, https://doi.org/10.5194/gh-71-121-2016, 2016.

Luethi, R., Phillips, M., and Lehning, M.: Estimating Non-Conductive Heat Flow Leading to Intra-Permafrost Talik Formation at the Ritigraben Rock Glacier (Western Swiss Alps), Permafrost and Periglacial Processes, 28, 183–194, https://doi.org/10.1002/ppp.1911, 2017.

Magnin, F. and Josnin, J.-Y.: Water Flows in Rock Wall Permafrost: A Numerical Approach Coupling Hydrological and Thermal Processes, Journal of Geophysical Research: Earth Surface, 126, e2021JF006 394, https://doi.org/10.1029/2021JF006394, 2021.

Magnin, F., Josnin, J.-Y., Ravanel, L., Pergaud, J., Pohl, B., and Deline, P.: Modelling rock wall permafrost degradation in the Mont Blanc massif from the LIA to the end of the 21st century, The Cryosphere, 11, 1813–1834, https://doi.org/10.5194/tc-11-1813-2017, 2017.

Magnin, F., Ravanel, L., Bodin, X., Deline, P., Malet, E., Krysiecki, J.-M., and Schoeneich, P.: Main results of permafrost monitoring in the French Alps through the PermaFrance network over the period 2010–2022, Permafrost and Periglacial Processes, 35, 3–23, https://doi.org/10.1002/ppp.2209, 2024.

Mamot, P., Weber, S., Schröder, T., and Krautblatter, M.: A temperature- and stress-controlled failure criterion for ice-filled permafrost rock joints, The Cryosphere, 12, 3333–3353, https://doi.org/10.5194/tc-12-3333-2018, 2018.

Marcer, M., Cicoira, A., Cusicanqui, D., Bodin, X., Echelard, T., Obregon, R., and Schoeneich, P.: Rock glaciers throughout the French Alps accelerated and destabilised since 1990 as air temperatures increased, Communications Earth & Environment, 2, 1–11, https://doi.org/10.1038/s43247-021-00150-6, 2021.

https://doi.org/10.5194/egusphere-2024-2652
Preprint. Discussion started: 15 October 2024

Marcer, M., Duvillard, P.-A., Tomaškovičová, S., Nielsen, S. R., Revil, A., and Ingeman-Nielsen, T.: Modelling present and future rock wall permafrost distribution in the Sisimiut mountain area, West Greenland, The Cryosphere, 18, 1753–1771, https://doi.org/10.5194/tc-18-1753-2024, 2024.

Matsuoka, N.: Diurnal freeze–thaw depth in rockwalls: Field measurements and theoretical considerations, Earth Surface Processes and Landforms, 19, 423–435, https://doi.org/10.1002/esp.3290190504, 1994.

Mellor, M.: Mechanical properties of rocks at low temperatures, in: 2nd International Conference on Permafrost, Yakutsk, pp. 334–344, International Permafrost Association, 1973.

Muller, S. W.: ... Permafrost, Or Permanently Frozen Ground: And Related Engineering Problems, Army map service, U. S. Army, 1945.

Murton, J., Kuras, O., Krautblatter, M., Cane, T., Tschofen, D., Uhlemann, S., Schober, S., and Watson, P.: Monitoring rock freezing and thawing by novel geoelectrical and acoustic techniques, J. Geophys. Res. Earth Surf., 121, 2309–2332, https://doi.org/10.1002/2016JF003948, 2016.

Murton, J. B. and French, H. M.: Cryostructures in permafrost, Tuktoyaktuk coastlands, western arctic Canada, Canadian Journal of Earth Sciences, 31, 737–747, https://doi.org/10.1139/e94-067, 1994.

Nicholson, L. and Benn, D. I.: Properties of natural supraglacial debris in relation to modelling sub-debris ice ablation, Earth Surface Processes and Landforms, 38, 490–501, https://doi.org/10.1002/esp.3299, 2013.

Offer, M., Weber, S., Krautblatter, M., Hartmeyer, I., and Keuschnig, M.: Pressurised water flow in fractured permafrost rocks revealed by joint electrical resistivity monitoring and borehole temperature analysis, EGUsphere, pp. 1–26, https://doi.org/10.5194/egusphere-2024-893, 2024.

PERMOS: Permafrost in Switzerland 2014/2015 to 2017/2018., Glaciological Report Permafrost No. 16-19 of the Cryospheric Commission of the Swiss Academy of Sciences, p. 117, https://doi.org/10.13093/permos-rep-2019-16-19, 2019.

PERMOS: PERMOS Database. Swiss Permafrost Monitoring Network, Davos and Fribourg, Switzerland., https://doi.org/10.13093/permos-2024-01, 2024.

Petersen, E.: ericivanpetersen/supraglacial_debris_heat_flux_JGR: JGR Paper Revision, https://zenodo.org/records/6574222, 2022.

Petersen, E., Hock, R., Fochesatto, G. J., and Anderson, L. S.: The Significance of Convection in Supraglacial Debris Revealed Through Novel Analysis of Thermistor Profiles, Journal of Geophysical Research: Earth Surface, 127, e2021JF006 520, https://doi.org/10.1029/2021JF006520, 2022.

Phillips, M., Haberkorn, A., Draebing, D., Krautblatter, M., Rhyner, H., and Kenner, R.: Seasonally intermittent water flow through deep fractures in an Alpine Rock Ridge: Gemsstock, Central Swiss Alps, Cold Regions Science and Technology, 125, 117 – 127, https://doi.org/https://doi.org/10.1016/j.coldregions.2016.02.010, 2016.

Phillips, M., Haberkorn, A., and Rhyner, H.: Snowpack characteristics on steep frozen rock slopes, Cold Regions Science and Technology, 141, 54 – 65, https://doi.org/https://doi.org/10.1016/j.coldregions.2017.05.010, 2017.

Phillips, M., Buchli, C., Weber, S., Boaga, J., Pavoni, M., and Bast, A.: Brief communication: Combining borehole temperature, borehole piezometer and cross-borehole electrical resistivity tomography measurements to investigate seasonal changes in ice-rich mountain permafrost, The Cryosphere, 17, 753–760, https://doi.org/10.5194/tc-17-753-2023, 2023.

Pogliotti, P., Cremonese, E., Morra di Cella, U., Gruber, S., and Giardino, M.: Thermal diffusivity variability in alpine permafrost rock walls, in: Pogliotti, P; Cremonese, E; Morra di Cella, U; Gruber, S; Giardino, M (2008). Thermal diffusivity variability in alpine permafrost rock walls. In: 9th International Conference on Permafrost, Fairbanks, Alaska, 29 June 2008 - 3 July 2008, 1427-1432., pp. 1427–1432, University of Zurich, Fairbanks, Alaska, https://doi.org/10.5167/uzh-3098, 2008.

https://doi.org/10.5194/egusphere-2024-2652
Preprint. Discussion started: 15 October 2024

Pogliotti, P., Cremonese, E., and Cella, U. M. d.: Warming Permafrost in the Western Alps: A Further Evidence of Elevation Dependent Warming?, Journal of Alpine Research | Revue de géographie alpine, https://doi.org/10.4000/rga.11784, 2023.

Pogrebiskiy, M. I. and Chernyshev, S. N.: Determination of the permeability of the frozen fissured rock massif in the vicinity of the Kolyma hydroelectric power station, Cold Regions Research and Engineering Laboratory – Draft translation, 634, 1–13, 1977.

Rist, A. and Phillips, M.: First results of investigations on hydrothermal processes within the active layer above alpine permafrost in steep terrain, Norsk Geografisk Tidsskrift - Norwegian Journal of Geography, 59, 177–183, https://doi.org/10.1080/00291950510020574, 2005.

Scherler, M., Hauck, C., Hoelzle, M., Stähli, M., and Völksch, I.: Meltwater infiltration into the frozen active layer at an alpine permafrost site, Permafrost and Periglacial Processes, 21, 325–334, https://doi.org/10.1002/ppp.694, 2010.

Scherler, M., Schneider, S., Hoelzle, M., and Hauck, C.: A two-sided approach to estimate heat transfer processes within the active layer of the Murtèl–Corvatsch rock glacier, Earth Surface Dynamics, 2, 141–154, https://doi.org/10.5194/esurf-2-141-2014, 2014.

Schuur, E. a. G., McGuire, A. D., Schädel, C., Grosse, G., Harden, J. W., Hayes, D. J., Hugelius, G., Koven, C. D., Kuhry, P., Lawrence, D. M., Natali, S. M., Olefeldt, D., Romanovsky, V. E., Schaefer, K., Turetsky, M. R., Treat, C. C., and Vonk, J. E.: Climate change and the permafrost carbon feedback, Nature, 520, 171–179, https://doi.org/10.1038/nature14338, 2015.

Smith, S. L., O'Neill, H. B., Isaksen, K., Noetzli, J., and Romanovsky, V. E.: The changing thermal state of permafrost, Nature Reviews Earth & Environment, 3, 10–23, https://doi.org/10.1038/s43017-021-00240-1, 2022.

Strauss, J., Fuchs, M., Hugelius, G., Miesner, F., Nitze, I., Opfergelt, S., Schuur, E., Treat, C., Turetsky, M., Yang, Y., and Grosse, G.: Organic matter storage and vulnerability in the permafrost domain, in: Reference Module in Earth Systems and Environmental Sciences, Elsevier, https://www.sciencedirect.com/science/article/pii/B9780323999311001641, 2024.

Stähli, M., Jansson, P.-E., and Lundin, L.-C.: Preferential Water Flow in a Frozen Soil — a Two-Domain Model Approach, Hydrological Processes, 10, 1305–1316, https://doi.org/10.1002/(SICI)1099-1085(199610)10:10<1305::AID-HYP462>3.0.CO;2-F, 1996.

Taber, S.: The mechanics of frost heaving, Journal of Geology, 38, 303–317, 1930.

Waples, D. and Waples, J.: A Review and Evaluation of Specific Heat Capacities of Rocks, Minerals, and Subsurface Fluids. Part 1: Minerals and Nonporous Rocks, Natural Resources Research, 13, 97–122, https://doi.org/10.1023/B:NARR.0000032647.41046.e7, 2004.

Weber, S.: Python3 module to infer thermal diffusivity from borehole temperature time series by simple linear regression analysis, numerical modeling, and analytical solution of the heat conduction equation, 2024.

Weber, S., Beutel, J., Da Forno, R., Geiger, A., Gruber, S., Gsell, T., Hasler, A., Keller, M., Lim, R., Limpach, P., Meyer, M., Talzi, I., Thiele, L., Tschudin, C., Vieli, A., Vonder Mühll, D., and Yücel, M.: A decade of detailed observations (2008–2018) in steep bedrock permafrost at the Matterhorn Hörnligrat (Zermatt, CH), Earth System Science Data, 11, 1203–1237, https://doi.org/10.5194/essd-11-1203-2019, 2019.

Wicky, J. and Hauck, C.: Numerical modelling of convective heat transport by air flow in permafrost talus slopes, The Cryosphere, 11, 1311–1325, https://doi.org/10.5194/tc-11-1311-2017, 2017.

Williams, P. and Smith, M.: The Frozen Earth: Fundamentals of Geocryology, Studies in Polar Research, Cambridge University Press, 1991.

Williams, P. J.: Unfrozen Water Content of Frozen Soils and Soil Moisture Suction, Géotechnique, 14, 231–246, https://doi.org/10.1680/geot.1964.14.3.231, 1964.

Yershov, E.: General geocryology (russian edition). PJ williams, technical editor, Cambridge University Press, 1998.

Zenklusen Mutter, E. and Phillips, M.: Active Layer Characteristics At Ten Borehole Sites In Alpine Permafrost Terrain, Switzerland, Permafrost and Periglacial Processes, 23, 138–151, https://doi.org/10.1002/ppp.1738, 2012.